1 French

Integrating abundance and diet data to improve inferences of food web dynamics

Jake M. Ferguson *[1], John B. Hopkins, III[2,3], and Briana H. Witteveen[4]

[1]Department of Fisheries, Wildlife and Conservation Biology, University of Minnesota, St Paul, MN, USA

[2]School of Biodiversity Conservation, Unity College, Unity, Maine, USA

[3]Division of Biological Sciences, Ecology, Behavior and Evolution Section, University of California San Diego, La Jolla, CA, USA

[4]School of Fisheries and Ocean Sciences, Alaska Sea Grant Marine Advisory Program, University of Alaska Fairbanks, Kodiak, AK, USA

*troutinthemilk@gmail.com
135 Skok Hall
2003 Upper Buford Circle
St. Paul, MN 55108

Abstract

1. Both population abundances and chemical tracers are useful tools for studying consumer-resource interactions. Food web models parameterized with abundances are often used to understand how interactions structure communities and to inform management decisions of complex ecological systems. Unfortunately, collecting abundance data to parameterize these models is often expensive and time-consuming. Another approach is to use chemical tracers to estimate the proportional diets of consumers by relating the tracers in their tissues to those found in their food sources. Although tracer data are often inexpensive to collect, these diet proportions provide little information on the per-capita consumption rates of consumers. Here, we show how coupling these data sources leads to better estimates of consumption rates.

2. Our modeling approach integrates traditional multispecies population abundance models with proportional diet estimates. We used simulations to determine whether integrated food web datasets were more informative than the standard abundance datasets and demonstrated the use of our integrated approach by estimating consumption rates of humpback whales (*Megaptera novaeangliae*) in the western Gulf of Alaska using abundances coupled with stable isotopes as a tracer.

3. Our simulations demonstrated that integrated models improved the ability to resolve alternative hypotheses about the functional response and yielded more precise parameter estimates relative to standard food web models. The integrated data approach was especially informative under low sample sizes or high process variance. Our application of the integrated modeling approach to humpback whales indicated that fish averaged about 25% of whale diets, though this proportion declined over the course of the study. We also found that traditional abundance model estimates of humpback whale consumption were non-estimable and that the integrated food web model led to estimable consumption rates.

4. Our results show that integrating stable isotopes and abundance datasets provides an exciting way forward for parameterizing multispecies models in data-limited systems.

We expect that future developments of these integrated approaches will extend current food web theory by allowing ecologists to study predation dynamics over seasonal time scales and at the individual level.

Keywords: integrated modeling | functional response | multispecies modeling | ecological tracers | stable isotopes | nonlinear time series | food web model

Background

Food web models allow ecologists to study how interspecific interactions drive the emergent complexity of communities (Thompson *et al.*, 2012). These models have revealed important relationships between biodiversity and ecosystem stability (May, 1972) and have practical applications for understanding the sensitivity of populations to the indirect effects of management decisions (Yodzis, 1998). Unfortunately, the difficulties inherent in parameterizing food webs limit both our ability to study the patterns of complex natural systems and the empirical applications of these models.

Collecting abundance data, which is commonly used to parameterize dynamic food web models (e.g., Ives *et al.*, 2003), is time-intensive and costly, as both predator and prey must be surveyed. The sampled populations are also often a subset of all the relevant biotic and abiotic factors in the system. Standard abundance models rely on using correlations between abundances through time to infer consumption rates. This approach has the potential to misidentify the influence of factors such as unsampled populations and climate factors as direct interactions between the sampled populations. A classic example of this phenomenon is apparent competition, in which two negatively correlated populations appear to be competing but instead are regulated by a consumer (Holt, 1977).

Bioenergetics modeling is another approach sometimes used to obtain consumption rates

for multispecies models. This method uses routinely collected data to partition the energy obtained from food to an individual's growth, metabolism, and waste products (Ney, 1993). In the few cases where validation of this approach is possible, estimates have routinely overestimated consumption, sometimes by several orders of magnitude (Chipps & Wahl, 2008). One previous study has coupled stable isotopes with bioenergetics models to determine prey consumption (Caut *et al.*, 2006). This approach, while useful, suffered from similar issues as standard bioenergetics models. Thus it is not clear that the bioenergetics approach is currently capable of producing reliable consumption rates for multispecies models.

Direct measurements of individual diet through the use of ecological tracers has proven to be a breakthrough in nutritional ecology (Phillips & Gregg, 2001; Galloway *et al.*, 2015; Kartzinel *et al.*, 2015). Stable isotopes, in particular, have been used to estimate the trophic position of species (Vander Zanden *et al.*, 1999), the proportional diets of consumers (Phillips & Gregg, 2001), and parameterize ecological networks (Yeakel *et al.*, 2012). Unfortunately, ecological tracers such as stable isotopes have been of limited use for understanding food web dynamics as they only measure diet proportions, which contain information on relative consumption, rather than the per-capita consumption values necessary to model the effect of predators on their prey.

In this study, we propose a new integrated modeling approach for parameterizing food webs. We show how to combine population abundance data collected at multiple trophic levels with proportional diets of consumers, derived from stable isotopes, to estimate the functional response of consumers. Combining multiple independent data sources mirrors integrated methods in population demography, which have successfully been used to parameterize complex models (Schaub *et al.*, 2007). Our approach constrains consumption estimates to be consistent with both the observed population dynamics and diets thus leading to predictions that are consistent with empirical dynamics.

Methods

We demonstrate our integrated modeling approach in two ways. First, we simulated the discrete-time dynamics of a consumer-resource interaction. We fit two types of models to these simulated datasets, abundance and integrated data models (described in detail below). This comparison allowed us to investigate how well each of the data models performed in both model selection and parameter estimation. Second, we fit the abundance and integrated models to data collected on humpback whales (*Megaptera novaeangliae*) and their prey in the western Gulf of Alaska using continuous-time models. These continuous-time models illustrate how to account for isotopic turnover in tissues occurring due to tissue replacement.

Models

Dynamical models

In this section, we describe two sets of models that can be used to describe how the processes of population growth and regulation as well as interspecific interactions drive community dynamics. The following section then describes how to connect these models to the data we collect.

The first set of difference equations is used to simulate time series of population abundances and of proportional diets. Discrete-time models may not be biologically realistic for many predator-prey processes they are often reasonable approximations, and for simulation studies they have the additional advantage that they are fast to simulate. The second set of models are continuous-time models of predation that we fit to a dataset of humpback whales and their prey. We use these continuous models to highlight how to the incorporate isotopic turnover of tissues.

Our system of difference equations contain a predator (P) and two prey (N_1, N_2):

$$\begin{aligned} P(t+1) &= \left[\varepsilon_1 N_1(t)\left(1-e^{-g_1(P(t),N_1(t),N_2(t))}\right)+\varepsilon_2 N_2(t)\left(1-e^{-g_2(P(t),N_1(t),N_2(t))}\right)+P(t)e^{-\mu}\right]e^{\sigma_P Z_P(t)} \\ N_1(t+1) &= \left[r_1 N_1(t)e^{-s_1 N_1(t)-g_1(P(t),N_1(t),N_2(t))}\right]e^{\sigma_1 Z_1(t)} \\ N_2(t+1) &= \left[r_2 N_2(t)e^{-s_2 N_2(t)-g_2(P(t),N_1(t),N_2(t))}\right]e^{\sigma_2 Z_2(t)}. \end{aligned} \tag{1}$$

The reproductive rate and strength of density dependence of each prey population is given by r and s, respectively. The density-independent mortality rate of the consumer is given by μ. Populations are subjected to process error at each time step, $Z(t)$, drawn from a standard normal distribution scaled by σ, the standard deviation. This error can be interpreted as temporal variation in the reproductive rate (Ferguson & Ponciano, 2015). The term, $1-e^{-g(P(t),N_1(t),N_2(t))}$, is the probability that an individual in the prey population does not escape consumption, while the efficiency of converting prey to new enemies is given by ε. Here we examined discrete-time equivalents of the type I and type II functional response. For a discrete-time type I response , $g(P(t),\, N_1(t),\, N_2(t))$ is given by $cP(t)$, where c is the per-capita consumption rate of the predator on the prey. For the type II response of the predator on the first prey population it is $\frac{c_1 P(t)}{1+c_1 h_1 N_1(t)+c_2 h_2 N_2(t)}$ (Mills & Getz, 1996) and the functional response for the second prey population is given by $g_2(P(t),\, N_1(t),\, N_2(t)) = \frac{c_2 P(t)}{1+c_2 h_2 N_2(t)+c_1 h_1 N_1(t)}$. Parameters used to simulate system 1 are given in Table 1.

A discrete-time system is appropriate for host-parasite interactions or predator-prey interactions when the sampling frequency is high relative to reproductive and consumption rates. However, continuous-time models may be more suitable for many other systems. We consider such a continuous-time process in our analysis of a data set of humpback whales and their prey (data described in Section). This system is

$$\begin{aligned} \frac{N_{\text{fish}}}{dt} &= r_{\text{fish}} N_{\text{fish}} - c_{\text{fish}} P N_{\text{fish}} \\ \frac{N_{\text{zoo}}}{dt} &= r_{\text{zoo}} N_{\text{zoo}} - c_{\text{zoo}} P N_{\text{zoo}}. \end{aligned} \tag{2}$$

The growth rates of fish and zooplankton are given by r_{fish} and r_{zoo}, while the per-capita consumption rates of fish and zooplankton by whales are given by c_{fish}. The yearly abundances of fish (N_{fish}), zooplankton (N_{zoo}), and whales (P) We did not build an explanatory model of within-year changes in humpback whales (P) because we assumed that this slow-growing population did not change throughout the feeding season and that changes between years may reflect factors other than limitation by prey, such as humpback whale's relatively recent release from commercial harvest (Gabriele *et al.*, 2017).

Data models

In this section, we describe how to fit food-web models using either abundance data or abundance data coupled with proportional diet data. Parameterizing these models with abundance data is a well-developed approach (see Ives *et al.*, 2003; Koen-Alonzo & Yodzis, 2005), however linking information about the proportional diets to these dynamics is novel. This link is achieved by understanding that the proportional diet is the total number of prey of a certain type consumed in a given time period relative to all of the predators consumption in that period. The number of consumed prey is given by the integral of the functional response.

Our first data model was informed using only the time series of abundances. This abundance model assumed that the population abundance at each time step followed a lognormal probability distribution representing fluctuations in the environment that were not accounted by our model. At each time step we conditioned abundance predictions on the previous time step, except for the first observation, which was only used to predict the second observation (following, Ferguson & Ponciano, 2014). In fitting the humpback whale dataset we also included the uncer-

tainty in estimated abundances (P, N_{fish}, and N_{zoo}) as observation error. The full specification of this state-space model is given in Appendix S1.

Our second approach is an integrated data model that utilizes both the abundance and proportional diet data to inform the models. The estimated dietary proportion data is linked to abundances by recognizing that this proportion can be written in terms of the consumed prey predicted by the functional response in the dynamical model. For the first prey population in a discrete-time system with type I functional response this proportion is, $p_1(t+1) = \frac{N_1(t)\left(1-e^{-c_1 P(t)}\right)}{N_1(t)\left(1-e^{-c_1 P(t)}\right)+N_2(t)\left(1-e^{-c_2 P(t)}\right)}$. We are particularly interested in applying this model to proportional diet data obtained from stable isotopes, where we may also need to account for isotopic turnover, the time required for the isotopic composition of an animal to reflect its diet (Vander Zanden *et al.*, 2015). In this approach the predicted diet at time $t+1$ is the integrated consumption of prey weighted by the isotopic turnover rate. This gives the diet proportion:

$$p_1(t+1) = \frac{\int_t^{t+1} e^{-\lambda(1-t)} f_1(P(t),\, N_1(t),\, N_2(t))\, dt}{\int_t^{t+1} e^{-\lambda(1-t)} f_1(P(t),\, N_1(t),\, N_2(t))\, dt + \int_t^{t+1} e^{-\lambda(1-t)} f_2(P(t),\, N_1(t),\, N_2(t))\, dt}, \tag{3}$$

where λ is the rate of isotopic turnover and the functions f_1 and f_2 are the functional responses of the predator for each of the two prey populations. When the turnover rate is very low such that $\lambda \approx 0$ this integral is the average proportional diet over the survey period. As the turnover rate increases this becomes a weighted average where more recently consumed items are more important.

We fit the predicted diet proportions to the observed diet proportions using a nonlinear logistic regression model with a mean given by the logit transform of the predicted proportion. The integrated log-likelihood is then the sum of the contributions from the logistic and the

abundance time series models.

Simulation study

We used simulated data generated from dynamical system 1 to test how informative the addition of proportional diet data is for parameter estimation and the ability to select the generating model from a set of alternative hypotheses. We simulated data under each of the type I and type II functional responses and fit both types of functional response as competing hypotheses to the generated data. In these simulations, we assumed that isotopic turnover could be ignored. This assumption is safe to make in scenarios when the turnover rate of the sampled tissue is approximately zero over the sampling period in, for example, tissues such as hair that record yearly diet. It could also be safe to make this assumption when changes in abundance between sampling periods are small. We made this assumption primarily to reduce the amount of computation needed for these simulations but incorporating turnover will not change the relative performance of these models.

Simulated time series were generated from system 1 for the type I and type II functional response using low ($\sigma = 0.1$), medium ($\sigma = 0.25$), and high ($\sigma = 0.5$) levels of process error, where we assumed the same value of σ for both prey and the predator populations. To generate datasets, we first simulated 500 time steps to ensure that the populations reach stationarity. We then selected sets of 10 to 100 observations from the end of the 500 samples, incrementing over this range by 10 to explore the effects of sample size on inference. For each combination of process variance/sample size/functional response we simulated 10,000 realizations of the process and fit the abundance and integrated data models to each dataset. We fit both type I and type II models to each simulated dataset. Models were fit in R using the nloptr package (Ypma, 2015) using a two-stage optimization procedure. We first used the global dividing rectangles algorithm (Gablonsky & Kelley, 2001), following this up with the Nelder-Mead algorithm (Box,

1965) to achieve convergence.

For each fitted dataset, we calculated the Bayesian Information Criterion (BIC) for the two competing functional response models to determine the most parsimonious model in the set (Burnham & Anderson, 2002). We then calculated the proportion of times that the generating model was selected by BIC using each data model for each process variance/sample size/functional response combination. We also calculated the bias of parameter estimates on the log-scale for each process variance/sample size/functional response combination. We note that the number of time points sampled is not equal to the sample size. For the abundance model with ten-time points, the total sample size is the 9-time points predicted by the model for each of the three populations sampled for a total sample size of 27. The integrated model has the sample size of the abundance data set plus the number of diet proportions used. For a sample of 10-time points, this corresponds to a total sample size of 36 (27 abundance samples and nine diet proportion samples). All data and code used for these analyses are provided on the Dryad Digital Repository (doi:10.5061/dryad.5q136q2).

Empirical study: the functional response of humpback whales

We used the abundance and integrated models to understand the impact of humpback whales on their prey populations in the western Gulf of Alaska. These migratory baleen whales play a major role in structuring this ecosystem through predation (Witteveen *et al.*, 2006, 2012; Wright *et al.*, 2015). Our dataset consisted of annual humpback abundances and the relative abundances of their zooplankton and fish prey estimated from past surveys (Wynne & Witteveen, 2015; Witteveen *et al.*, 2015). We also estimated the proportional contributions of these major food sources to the diets of whales each year using the IsotopeR stable isotope mixing model (Hopkins & Ferguson, 2012). In particular, we used carbon ($^{13}C/^{12}C$) and nitrogen ($^{15}N/^{14}N$) stable isotope ratios (expressed as $\delta^{13}C$ and $\delta^{15}N$) from individual whales (n=114), fish (n=211),

and zooplankton (n=36) to estimate dietary parameters. We then estimated consumption rates of humpback whales using both the standard abundance model and the integrated model and compared the results.

Wynne & Witteveen (2015) estimated whale abundances from photographs of individual whales taken during annual vessel surveys from 2004, 2005, 2007, and 2012-2014. We used the estimated abundances from the eastern portion of the study area because the relative densities of zooplankton and fish were also collected in this region during vessel surveys using acoustic volume backscatter; the relative frequency response was used to estimate relative zooplankton and fish densities (Wynne & Witteveen, 2015; Witteveen *et al.*, 2015). These densities, described here as population indices, are proportional to the total relative abundance of each prey population.

We estimated the proportional assimilated diets of humpback whales using carbon (^{13}C/^{12}C) and nitrogen (^{15}N/^{14}N) stable isotope ratios (expressed as $\delta^{13}\mathrm{C}$ and $\delta^{15}\mathrm{N}$) derived from 119 skin samples (114 individuals) collected from adults ($n = 80$), juveniles ($n = 4$), and whales of unknown age (but not calves that were dependent on their mothers; $n = 35$). Skin samples of whales were collected using a pneumatic-dart system from June through September between 2004-2014 (Wright *et al.*, 2015). We also used stable isotope values for fish (capelin, *Mallotus villosus*: $n = 84$; Pacific herring, *Clupea pallasii*: $n = 85$; Alaska pollock, *Theragra chalcogramma*: $n = 42$) collected during vessel surveys in 2012 in areas with the highest acoustic backscatter densities. Sampling was done using a mid-water trawl net with 22 mm mesh cod-end liner (following Witteveen *et al.*, 2012). Zooplankton were also collected using a 75 cm diameter twin-ring net (500/1000 μmesh) and separated into taxonomic groups though not identified to species (e.g., euphausiids and copepods) (euphausiids: $n = 14$; copepods: $n = 22$) as reported in Witteveen & Wynne (2016).

We added stable isotope discrimination factors (small offsets of stable isotope values be-

tween dietary sources and animal tissues) to the isotope values of each sampled food. In particular, we added the mean discrimination factors for skin of fin whales that fed on krill (Δ^{13}C = 1.3 $\pm$ 0.4; Δ^{15}N = 2.8 $\pm$ 0.3; (Borrell *et al.*, 2012)) to the stable isotope values of sampled zooplankton, and discrimination factors for killer whale (*Orcinus orca*) and bottlenose dolphin (*Tursiops truncates*) that fed on fish diets (Δ^{13}C = 2.4; Δ^{15}N = 3.2, (Caut *et al.*, 2011)) to the stable isotope values of fish sampled in this study.

We used IsotopeR (Ferguson & Hopkins, 2013) to estimate the isotopic mixing space and the proportional diets (fish and zooplankton) of whales each year. We ran 3 MCMC chains with a burn-in of 10^3 draws followed by 10^4 draws from the posterior. We checked graphical and other diagnostic output for evidence of convergence. We reported the mean, 1 SD, median, and 95% credible interval for each marginal posterior density distribution (i.e., proportional dietary contribution) for each major food source (Dryad Digital Repository DOI here upon acceptance).

Stable isotope mixing models are used to measure the proportional contributions of digestible biomass from each prey item to consumers (Phillips, 2012), whereas population dynamics are often defined in terms of abundances. To get the proportional diet on the same scale as the per-capita consumption, we converted the per-capita consumption rate from a measure of consumed prey individuals to a measure of consumed biomass. First, we calculated the consumed biomass of each prey item by multiplying the total number of consumed prey (C) between observations $\left(C = \int_t^{t+1} e^{-\lambda(1-x)} f(P(x),\, N_1(x),\, N_2(x))\, dx\right)$ by the average prey biomass (b). We then corrected the number consumed by the digestibility (D) to get the consumed biomass of each prey item $D \cdot b \cdot C$. Prey digestion of zooplankton was assumed to be 93%, consistent with minke whales (*Balaenoptera acutorostrata*) (Martensson *et al.*, 1994), and 100% for fish, as measured in some species of dolphin (Sekiguchi & Best, 1997).

Parameter estimation

We used both the abundance and integrated data models to estimate the consumption of prey by humpback whales. We used n-step predictions (where n is the number of years between observations) because annual data were not available for the whole study period. We used 1-step predictions in 2005, 2013, and 2014; a 2-step prediction for 2007; and a 5-step prediction for 2012. We fit the type I functional response defined in system 2 to the abundances and assumed that predicted populations followed a lognormal distribution. To incorporate the known uncertainty in estimated whale, fish, and zooplankton densities, we used a Bayesian model. All estimation was done in JAGS (Plummer, 2012) and code and data to reproduce the analysis are available on the Dryad Digital Repository (doi:10.5061/dryad.5q136q2).

In the integrated model, we incorporated isotopic turnover of humpback whales using equation 3. Past work has suggested that equilibration of stable isotopes from food into whale skin can take anywhere from 7 days (Witteveen *et al.*, 2011; Todd *et al.*, 1997) to 2 months (Hicks *et al.*, 1985). We assumed that these turnover times were equal to the half-life $(\ln(2)/\lambda)$ of the tissue and ran our models with both $\lambda = 7/365$ and $\lambda = 60/365$.

Results

Simulation study

Under all simulation conditions, integrated models performed better than abundance models at selecting the generating model (Figure 2). The ability to choose the generating model was dependent on the sample size, process variance, and generating model. As expected, we found that higher variation in the data tended to reduce the ability to detect the generating model, whereas larger sample sizes increased capacity to select the generating model. An interest-

ing exception to this pattern was the poor performance of the abundance model with type II functional response under low sample size and process variance. In this case model selection performed worse than more variable scenarios because there was not enough variation in the data to observe fluctuations in the functional response. When the generating model was the type I functional response, there was little difference between the data models with the generating model selected over 96% of the time for all simulation conditions (Figure 2a). When the generating model was the type II functional response, there was a large difference between the data models' ability to select the generating model. For example, in a sample of 10-time points with low process variance the abundance data model selected the generating model 26% of the time while the integrated data model selected the generating model 80% of the time (Figure 2b). As the sample size increased, the performance differential of the data models decreased.

We report results of estimator bias under the type II functional response and high process variance (Figure 3). We note that the other simulation conditions led to similar conclusions, though performance differences decreased with lower process variance. We found that estimator bias was less for the integrated data model than the abundance data model with the same number of time points sampled (Figure 3) except for a couple of cases discussed below. The estimates of the half-saturation coefficient for prey 1 (h_1) and both of the consumption rates $(c_1,\, c_2)$ improved the most under the integrated model. Interesting h_2 did not improve with the integrated model even though we saw improvements in h_1 and c_2. We also detected improvements in a number parameters that were not directly related to predator diet (e.g., r_1, s_1, Figure 3), even though the integrated model did not contain any direct information about these parameters. These improvements occur because well-estimated functional response parameters allow for the identification of other population parameters.

We did find some significant issues in the sampling distributions of the diet efficiencies and predator mortality terms $(\varepsilon_1,\, \varepsilon_2,\, \mu)$. The sampling distribution of these parameters was mul-

timodal (Figure S1), though we found that the primary mode of the sampling distribution did appear to be a reasonable estimator. It is likely that multimodality occurs because these parameters are additive functions of the predator population in system 1; therefore, they can be difficult to identify statistically. Approaches to deal with this issue are to place biologically plausible constraints on the range of diet efficiencies or to determine reasonable starting points for parameter values from the literature then use local optimization instead of a global algorithm. We performed a small set of secondary simulations that indicate reasonable constraints on parameters removes the multimodal behavior and lead to estimates that behave similarly to others in the study.

Empirical Study: Trophic dynamics of humpback whales

Abundance and proportional diets

Abundance estimates of the humpback whale population ranged from 1665 whales in 2004 to 551 in 2012 (Figure 4), with a coefficient of variation of 0.41 over the course of the study. The population indices for fish and zooplankton were also highly variable with coefficients of variation of 0.69 and 1.08, respectively (Figure 4).

The stable isotope values measured from whale skin, fish, and zooplankton data and sources are illustrated in Figure 1. Using Kruskal–Wallis tests, we found that unlike $\delta^{15}N$ ($H = 7.792$, $df = 5$, $p = 0.1681$), $\delta^{13}C$ values were different among years ($H = 49.3747$, $df = 5$, $p < 0.005$; Figure S1). Interestingly, $\delta^{13}C$ values seemed to decrease in a step-wise fashion (Figure S2). We also learned that both $\delta^{13}C$ and $\delta^{15}N$ values were lower for zooplankton ($\delta^{13}C$: -18.2 ± 1.0; $\delta^{15}N$: 11.9 ± 0.9) than fish ($\delta^{13}C$: -15.4 ± 0.9; $\delta^{15}N$: 15.7 ± 1.0) (Figure 1). We used these stable isotope data to estimate the diets of whales through time using IsotopeR and found that the annual mean contribution of fish varied substantially in the diets of

whales from 45% in 2004 to 4% in 2014 (Figure 4 inset).

Parameter estimation

The abundance data model had 15 observations for a system with six parameters. Incorporating diet data with the integrated data model increased the number of observations by 40% to 20 observations. Here, we report estimates assuming that the tissue half-life is 7 days, though we note increasing upper limit on the estimate of turnover 60 days does not alter the point estimates. We estimated the consumption rate of fish (c_{fish}) in our abundance model as $\hat{c}_{\text{fish}} = 5.06 \cdot 10^{-10}$ versus the estimate from the integrated model of $\hat{c}_{\text{fish}} = 3.85 \cdot 10^{-13}$. Both estimates have credible intervals that extend to 0 (Figure 5a) and are thus weakly estimable (*sensu* Ponciano *et al.*, 2012), with a flat posterior distribution. The estimates of the consumption rate on zooplankton for the abundance data model estimated $\hat{c}_{\text{zoo}} = 1.34 \cdot 10^{-10}$ versus $1.10 \cdot 10^{-6}$ for the integrated data model. Incorporating the diet estimates in the integrated model led to this parameter becoming estimable (Figure 5b).

Discussion

We developed a framework to parameterize food web models by integrating proportional diet and population abundance data. The primary advantage of using proportional diet information is that it provides an independent measure of consumption, a quantity that dynamical models have estimated by relying on correlations between populations. The simulation component of our study demonstrated that the integrated approach yields more precise parameter estimates and can better distinguish competing between hypotheses relative to standard abundance models. Because the integrated food web model uses more data than conventional methods improved performance was not surprising; however, we were surprised by the substantial degree

of improvement in the integrated models for datasets with low sample size and low process variance or moderate sample sizes with high process variance (Figure 2). Our empirical example highlighted how incorporating diet information can resolve parameters that cannot be precisely estimated using abundance data (Figure 5).

Based on the results of our stable isotope analysis, around 25% of the humpback whale diet is composed of fish, though this can vary from over 40% in some years to under 5% in others (Figure 4). Previous diet estimates, calculated using stable isotope mixing models, found a larger proportion of fish in humpback whale diets (Witteveen *et al.*, 2012; Wright, 2014). We attribute this discrepancy to different analytical procedures. For instance, we used skin discrimination factors for marine mammals that fed on these food sources (fish and krill), rather than those associated with other tissues and foods. We also structured our mixing models differently than past studies by grouping sampled foods into two main food sources whereas Witteveen *et al.* (2012) estimated the diets of whales using 2-isotope systems and either 5 or 9 sources.

Although we applied the best analytical practices available in our analysis of whale diets, several limitations may have influenced the results of our case study. First, our model did not explicitly account for the migratory life history of whales. Stable isotopes from food acquired in the winter breeding ground could be influencing the measurements made in Alaska if the isotopic turnover time is on the long end of the estimated range (between 7 and 60 days). In addition, we did not include any direct interactions between fish and zooplankton due to the constraint imposed by having a small sample size. Finally, our analysis assumed that the isotope values of whale's prey did not significantly vary through time. It is known that the isotope values of fishes can vary considerably from year to year, sometimes as much as up to 2‰ in Nitrogen and Carbon (Kurle *et al.*, 2011). Accounting for such variation will be a significant step in refining the estimates obtained here. Thus, while we do not consider our models sufficiently sophisticated for making accurate predictions of system dynamics, our

analysis showed that integrative food web models do have significant advantages over standard abundance approaches.

We focused this study on three-species trophic interactions. When applying integrated food web models to larger food webs, stable isotope methods may be unable to uniquely estimate the dietary proportions of generalist consumers (Hopkins & Kurle, 2016). This nonestimability occurs when the number of sources exceeds the number of isotope tracers commonly used in ecology (^{2}H, ^{15}O, ^{13}C, ^{15}N, and ^{34}S) by more than one (Phillips & Gregg, 2003). Including informative priors in the mixing model (Chiaradia *et al.*, 2014) or using prey abundance data to weight source estimates (Yeakel *et al.*, 2011) have both been used to circumvent this analytical limitation. Another promising method is to supplement stable isotopes with fatty acid data, a technique that can extend the number of ecological tracers for systems with many dietary sources (Galloway *et al.*, 2015).

As a general rule of thumb for designing integrated multispecies studies, we advise sampling both abundance and tissues at a frequency defined by the population with the fastest turnover. This study design will generate datasets with sufficient fluctuations in density that the response to predation can be observed without increasing effort by surveying populations that have not had time to respond to the effects of predation. In cases where the stable isotopes are being collected retroactively, e.g., through museum specimens, we suggest starting with asensitivity analysis of the multispecies abundance model to determine which interactions are the most critical to answering your scientific question. Then place most effort on collecting and analyzing the appropriate tissues to inform those interactions.

We believe that integrated food web models show promise for ecologists interested in studying new facets of multispecies dynamics. The ability of ecological tracers to detect differences in consumption at the individual level could lead to new models that explore the impacts of group, or even individual heterogeneity on food web dynamics. For example, integrated data

models could be used to explore the heterogeneity of diet over the life history of individuals. This heterogeneity may play a substantial role in compartmentalizing feeding interactions and thus buffering the propagating effects of a single population going extinct (Stouffer & Bascompte, 2011) and thus in determining community stability (May, 2001; Ferguson *et al.*, 2012), though there is currently very little data available to test this hypothesis.

It is difficult to accurately determine the functional response without experiments (e.g., Arditi *et al.*, 1991) or extensive behavioral field studies (e.g., Fryxell *et al.*, 2007; Novak & Wootton, 2008). However, the functional response determines a number of key ecosystem properties such as whether trophic cascades occur and how systems will respond to enrichment (Arditi & Ginzburg, 2012). Here we show that combining existing data sources using integrated methods is one way forwards for accurately parameterizing complex, empirical food web dynamics. New methods to directly observe ecological interactions may allow ecologists to accurately model the functional response and lead to new insights into the role of predation in food webs.

Data accessibility: Data and code for analysis of the humpback whales and their prey is available from Dryad: doi:10.5061/dryad.5q136q2.

Authors' contributions: JMF and JBH conceived the study; JMF led the analysis and wrote the first draft of the manuscript. JBH contributed substantial revisions and performed the stable isotope analysis. BHW provided data and feedback on the manuscript.

Acknowledgements: The majority of this work was conducted while JMF was a Postdoctoral Fellow at the National Institute for Mathematical and Biological Synthesis (NIMBIOS), an Institute sponsored by the National Science Foundation through NSF Award #DBI-1300426 with additional support from The University of Tennessee, Knoxville. JBH was assisted by attendance as a Short-term Visitor at the NIMBIOS, through NSF Award #DBI-1300426, with additional support from The University of Tennessee, Knoxville. Whale data was collected

under NMFS Federal Research Permits #1049-1718 and 14296 and University of Alaska Fairbanks IACUC protocols 140171 and 140169. Funding for whale and prey data collection was provided to the Gulf Apex Predator Prey project by NOAA Grants. We would like to thank an anonymous reviewer and the associate editor for their feedback that improved the manuscript.

Data accessibility: Data available from the Dryad Digital Repository (link available upon acceptance).

References

Arditi, R. & Ginzburg, L. (2012) *How species interact: altering the standard view on trophic ecology*, volume 88. Oxford University Press, Oxford.

Arditi, R., Perrin, N. & Saiah, H. (1991) Functional Responses and Heterogeneities : An Experimental Test with Cladocerans. *Oikos*, **60**, 69–75.

Borrell, A., Abad-Oliva, N., Gómez-Campos, E., Giménez, J. & Aguilar, A. (2012) Discrimination of stable isotopes in fin whale tissues and application to diet assessment in cetaceans. *Rapid Communications in Mass Spectrometry*, **26**, 1596–602.

Box, M.J. (1965) A new method of constrained optimization and a comparison with other methods. *The Computer Journal*, **8**, 42–52.

Burnham, K.P. & Anderson, D.R. (2002) *Model Selection and Multimodel Inference: A Practical Information-theoretic Approach*. Springer.

Caut, S., Laran, S., Garcia-Hartmann, E. & Das, K. (2011) Stable isotopes of captive cetaceans (killer whales and bottlenose dolphins). *Journal of Experimental Biology*, **214**, 538–545.

449 Caut, S., Roemer, G.W.., Donlan, C..J. & Courchamp, F. (2006) Coupling Stable Isotopes with
450 Bioenergetics to Estimate Interspecific Interactions. *Ecological Applications*, **16**, 1893–1900.

451 Chiaradia, A., Forero, M.G., McInnes, J.C. & Ramírez, F. (2014) Searching for the true diet
452 of marine predators: incorporating Bayesian priors into stable isotope mixing models. *PLoS*
453 *ONE*, **9**, e92665.

454 Chipps, S.R. & Wahl, D.H. (2008) Bioenergetics modeling in the 21st century: reviewing new
455 insights and revisiting old constraints. *Transactions of the American Fisheries Society*, **137**,
456 298–313.

457 Ferguson, J. & Hopkins, J.B. (2013) IsotopeR: Stable isotope analysis.

458 Ferguson, J.M. & Ponciano, J.M. (2015) Evidence and implications of higher-order scaling
459 in the environmental variation of animal population growth. *Proceedings of the National*
460 *Academy of Sciences*, **112**, 2782–2787.

461 Ferguson, J.M. & Ponciano, J.M. (2014) Predicting the process of extinction in experimental
462 microcosms and accounting for interspecific interactions in single-species time series. *Ecol-*
463 *ogy Letters*, **17**, 251–259.

464 Ferguson, J.M., Taper, M.L., Guy, C.S. & Syslo, J.M. (2012) Mechanisms of coexistence be-
465 tween native bull trout (Salvelinus confluentus) and non-native lake trout (Salvelinus na-
466 maycush): inferences from pattern-oriented modeling. *Canadian Journal of Fisheries and*
467 *Aquatic Sciences*, **769**, 755–769.

468 Fryxell, J.M., Mosser, A., Sinclair, A.R.E. & Packer, C. (2007) Group formation stabilizes
469 predator-prey dynamics. *Nature*, **449**, 1041–3.

Gablonsky, J.M. & Kelley, C.T. (2001) A locally-biased form of the DIRECT algorithm. *Journal of Global Optimization*, **21**, 27–37.

Gabriele, C.M., Neilson, J.L., Straley, J.M., Baker, C.S., Cedarleaf, J.A. & Saracco, J.F. (2017) Natural history, population dynamics, and habitat use of humpback whales over 30 years on an Alaska feeding ground. *Ecosphere*, **8**.

Galloway, A.W.E., Brett, M.T., Holtgrieve, G.W., Ward, E.J., Ballantyne, A.P., Burns, C.W., Kainz, M.J., Müller-Navarra, D.C., Persson, J., Ravet, J.L., Strandberg, U., Taipale, S.J. & Alhgren, G. (2015) A Fatty Acid Based Bayesian Approach for Inferring Diet in Aquatic Consumers. *PLoS ONE*, **10**, e0129723.

Hicks, B.D., Aubin, D.J.S., Geraci, J.R. & Brown, W.R. (1985) Epidermal growth in the bottlenose dolphin, Tursiops truncatus. *Journal of Investigative Dermatology*, **85**, 60–63.

Holt, R.D. (1977) Predation, Apparent Competition, and the Structure of Prey Communities. *Theoretical Population Biology*, **12**, 197–229.

Hopkins, J.B. & Ferguson, J.M. (2012) Estimating the Diets of Animals Using Stable Isotopes and a Comprehensive Bayesian Mixing Model. *PLoS ONE*, **7**, 1–13.

Hopkins, J.B. & Kurle, C.M. (2016) Measuring the realized niches of animals using stable isotopes: from rats to bears. *Methods in Ecology and Evolution*, **7**, 210–221.

Ives, A.R., Dennis, B., Cottingham, K.L. & Carpenter, S.R. (2003) Estimating Community Stability and Ecological Interactions From Time-Series Data. *Ecological Monographs*, **73**, 301–330.

Kartzinel, T.R., Chen, P.a., Coverdale, T.C., Erickson, D.L., Kress, W.J., Kuzmina, M.L., Rubenstein, D.I., Wang, W. & Pringle, R.M. (2015) DNA metabarcoding illuminates di-

etary niche partitioning by African large herbivores. *Proceedings of the National Academy of Sciences*, **112**, 8019–8024.

Koen-Alonzo, M. & Yodzis, P. (2005) Multispecies modeling of some components of the northern and central Patagonia marine community, Argentina. *Canadian Journal of Fisheries and Aquatic Sciences*, **62**.

Kurle, C.M., Sinclair, E.H., Edwards, A.E. & Gudmundson, C.J. (2011) Temporal and spatial variation in the δ15N and δ13C values of fish and squid from Alaskan waters. *Marine Biology*, **158**, 2389–2404.

Martensson, P.E., Nordoy, E.S. & Blix, A.S. (1994) Digestibility of krill (Euphausia superba and Thysanoessa sp.) in minke whales (Balaenoptera acutorostrata) and crabeater seals (Lobodon carcinophagus). *British Journal of Nutrition*, **72**, 713–716.

May, R.M. (1972) Will a large complex system be stable? *Nature*, **238**, 413–414.

May, R.M. (2001) *Stability and Complexity in Model Ecosystems*, volume 6 of *Monographs in Population Biology*. Princeton University Press, Princeton, New Jersey.

Mills, N. & Getz, W. (1996) Modelling the biological control of insect pests: a review of host-parasitoid models. *Ecological Modelling*, **92**, 121–143.

Ney, J.J. (1993) Bioenergetics Modeling Today: Growing Pains on the Cutting Edge. *Transactions of the American Fisheries Society*, **122**, 736–748.

Novak, M. & Wootton, J.T. (2008) Estimating nonlinear interaction strengths: An observation-based method for species-rich food webs. *Ecology*, **89**, 2083–2089.

Phillips, D.L. (2012) Converting isotope values to diet composition: the use of mixing models. *Journal of Mammalogy*, **93**, 342–352.

514 Phillips, D.L. & Gregg, J.W. (2001) Uncertainty in source partitioning using stable isotopes.
515 *Oecologia*, **127**, 171–179.

516 Phillips, D.L. & Gregg, J.W. (2003) Source partitioning using stable isotopes: coping with too
517 many sources. *Oecologia*, **136**, 261–9.

518 Plummer, M. (2012) JAGS Version 3.3. 0 user manual. Technical report, International Agency
519 for Research on Cancer, Lyon, France.

520 Ponciano, J.M., Burleigh, J.G., Braun, E.L. & Taper, M.L. (2012) Assessing parameter identifi-
521 ability in phylogenetic models using data cloning. *Systematic Biology*, **61**, 955–72.

522 Schaub, M., Gimenez, O., Sierro, A. & Arlettaz, R. (2007) Use of integrated modeling to en-
523 hance estimates of population dynamics obtained from limited data. *Conservation Biology*,
524 **21**, 945–55.

525 Sekiguchi, K. & Best, P.B. (1997) In vitro digestibility of some prey species of dolphins. *Fishery*
526 *Bulletin*, **95**, 386–393.

527 Stouffer, D.B. & Bascompte, J. (2011) Compartmentalization increases food-web persistence.
528 *Proceedings of the National Academy of Sciences*, **108**, 3648–3652.

529 Thompson, R.M., Brose, U., Dunne, J.A., Hall, R.O., Hladyz, S., Kitching, R.L., Martinez,
530 N.D., Rantala, H., Romanuk, T.N., Stouffer, D.B. & Tylianakis, J.M. (2012) Food webs:
531 reconciling the structure and function of biodiversity. *Trends in Ecology & Evolution*, **27**,
532 689–697.

533 Todd, S., Ostrom, P., Lien, J. & Abrajano, J. (1997) Use of biopsy samples of humpback whale
534 (Megaptera novaeangliae) skin for stable isotope (δ13C) determination. *Journal of Northwest*
535 *Atlantic Fishery Science*, **22**, 71–76.

536 Vander Zanden, M.J., Casselman, J.M. & Rasmussen, J.B. (1999) Stable isotope evidence for
537 the food web consequences of species invasions in lakes. *Nature*, **401**, 464–467.

538 Vander Zanden, M.J., Clayton, M.K., Moody, E.K., Solomon, C.T. & Weidel, B.C. (2015)
539 Stable isotope turnover and half-life in animal tissues: a literature synthesis. *PloS ONE*, **10**,
540 e0116182.

541 Witteveen, B.H. & Wynne, K.M. (2016) Trophic niche partitioning and diet composition of
542 sympatric fin (Balaenoptera physalus) and humpback whales (Megaptera novaeangliae) in
543 the Gulf of Alaska revealed through stable isotope analysis. *Marine Mammal Science*, **32**,
544 1319–1339.

545 Witteveen, B., Foy, R. & Wynne, K. (2006) The effect of predation (current and historical) by
546 humpback whales (Megaptera novaeangliae) on fish abundance near Kodiak Island, Alaska.
547 *Fishery Bulletin*, pp. 10–20.

548 Witteveen, B.H., De Robertis, A., Guo, L. & Wynne, K.M. (2015) Using dive behavior and
549 active acoustics to assess prey use and partitioning by fin and humpback whales near Kodiak
550 Island, Alaska. *Marine Mammal Science*, **31**, 255–278.

551 Witteveen, B.H., Worthy, G.A.J., Wynne, K.M., Hirons, A.C., Andrews, A.G. & Markel,
552 R.W. (2011) Trophic Levels of North Pacific Humpback Whales (Megaptera novaeangliae)
553 Through Analysis of Stable Isotopes: Implications on Prey and Resource Quality. *Aquatic*
554 *Mammals*, **37**, 101–110.

555 Witteveen, B.H., Worthy, G.a.J., Foy, R.J. & Wynne, K.M. (2012) Modeling the diet of hump-
556 back whales: An approach using stable carbon and nitrogen isotopes in a Bayesian mixing
557 model. *Marine Mammal Science*, **28**, E233–E250.

Wright, D.L. (2014) *Variability in foraging by humpback whales (Megaptera novaengliae) on the Kodiak, AK, feeding ground.* Ph.d. dissertation, University of Alaska Fairbanks.

Wright, D.L., Witteveen, B., Wynne, K. & Horstmann-Dehn, L. (2015) Evidence of two subaggregations of humpback whales on the Kodiak, Alaska, feeding ground revealed from stable isotope analysis. *Marine Mammal Science*, **31**, 1378–1400.

Wynne, K.M. & Witteveen, B.H. (2015) Comprehensive Final Report for the role of balaenopterids in structuring Kodiak's marine ecosystem. Technical report.

Yeakel, J.D., Guimarães, P.R., Novak, M., Fox-Dobbs, K., Koch, P.L., Guimaraes, P.R., Novak, M., Fox-Dobbs, K. & Koch, P.L. (2012) Probabilistic patterns of interaction: the effects of link-strength variability on food web structure. *Journal of The Royal Society Interface*, **9**, 3219–3228.

Yeakel, J.D., Novak, M., Guimarães, P.R., Dominy, N.J., Koch, P.L., Ward, E.J., Moore, J.W. & Semmens, B.X. (2011) Merging Resource Availability with Isotope Mixing Models: The Role of Neutral Interaction Assumptions. *PLoS ONE*, **6**, e22015.

Yodzis, P. (1998) Local trophodynamics and the interaction of marine mammals and fisheries in the Benguela ecosystem. *Journal of Animal Ecology*, **67**, 635–658.

Ypma, J. (2015) nloptr: R Interface to NLopt.

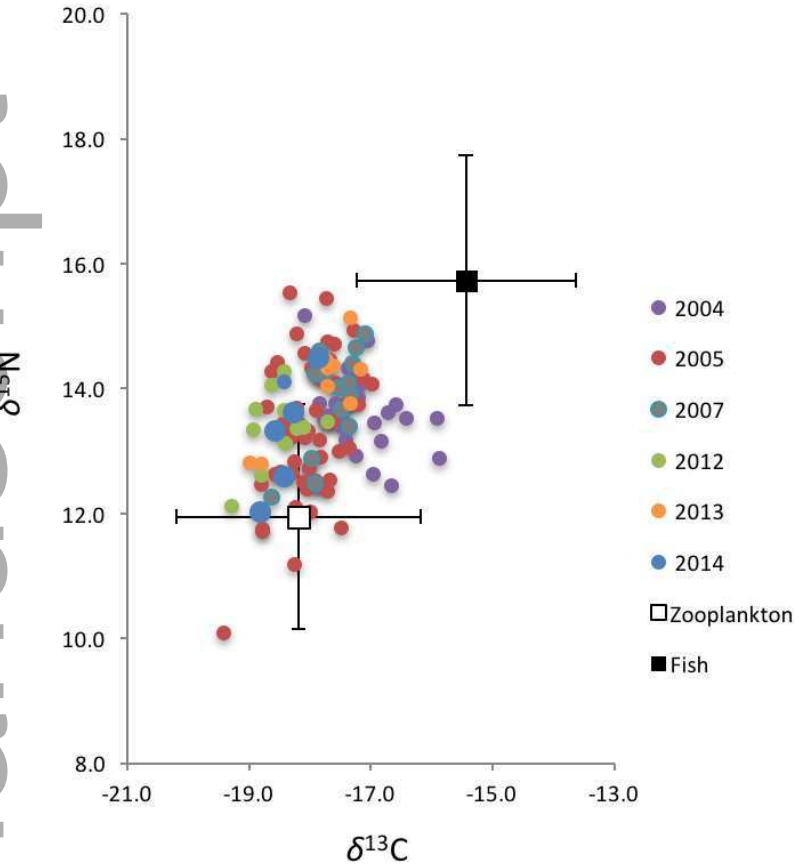

Figure 1: Isotope values ($\delta^{13}C$, $\delta^{15}N$) derived from the skin of humpback whales and their prey (corrected for isotopic discrimination). Each color denotes a different sampling year and error bars denote 2 standard deviations.

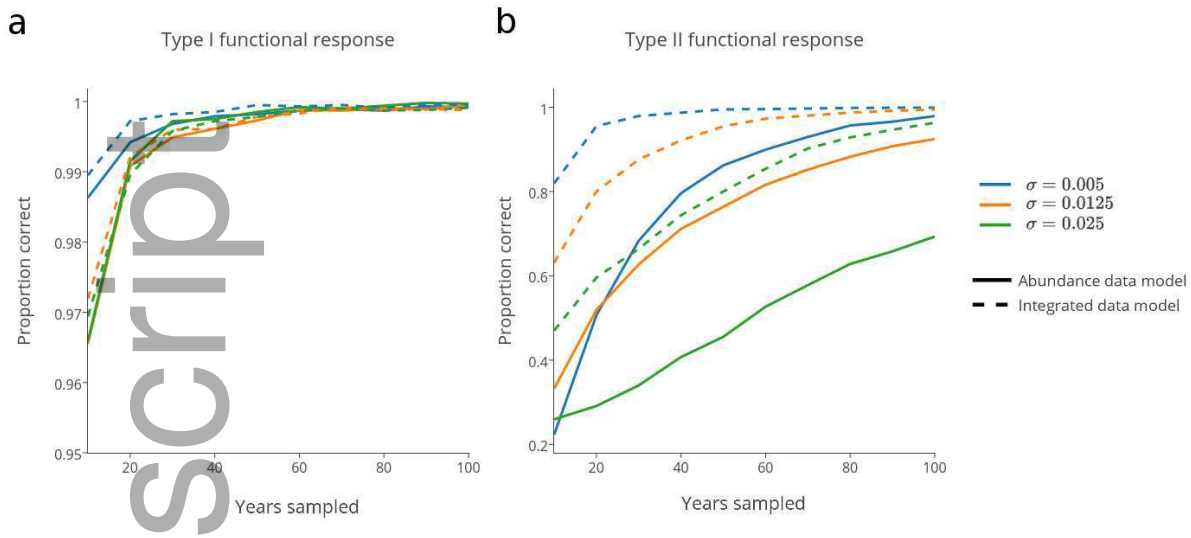

Figure 2: Proportion of correct functional response selections made using BIC for each data model (solid lines for abundance data model, dashed lines for integrated data models). The x-axis is given in terms of the number of sample points used for the estimation, where samples occur yearly. In panel **a** the generating model is a type I functional response and panel **b** is for when the generating model is a type II functional response.

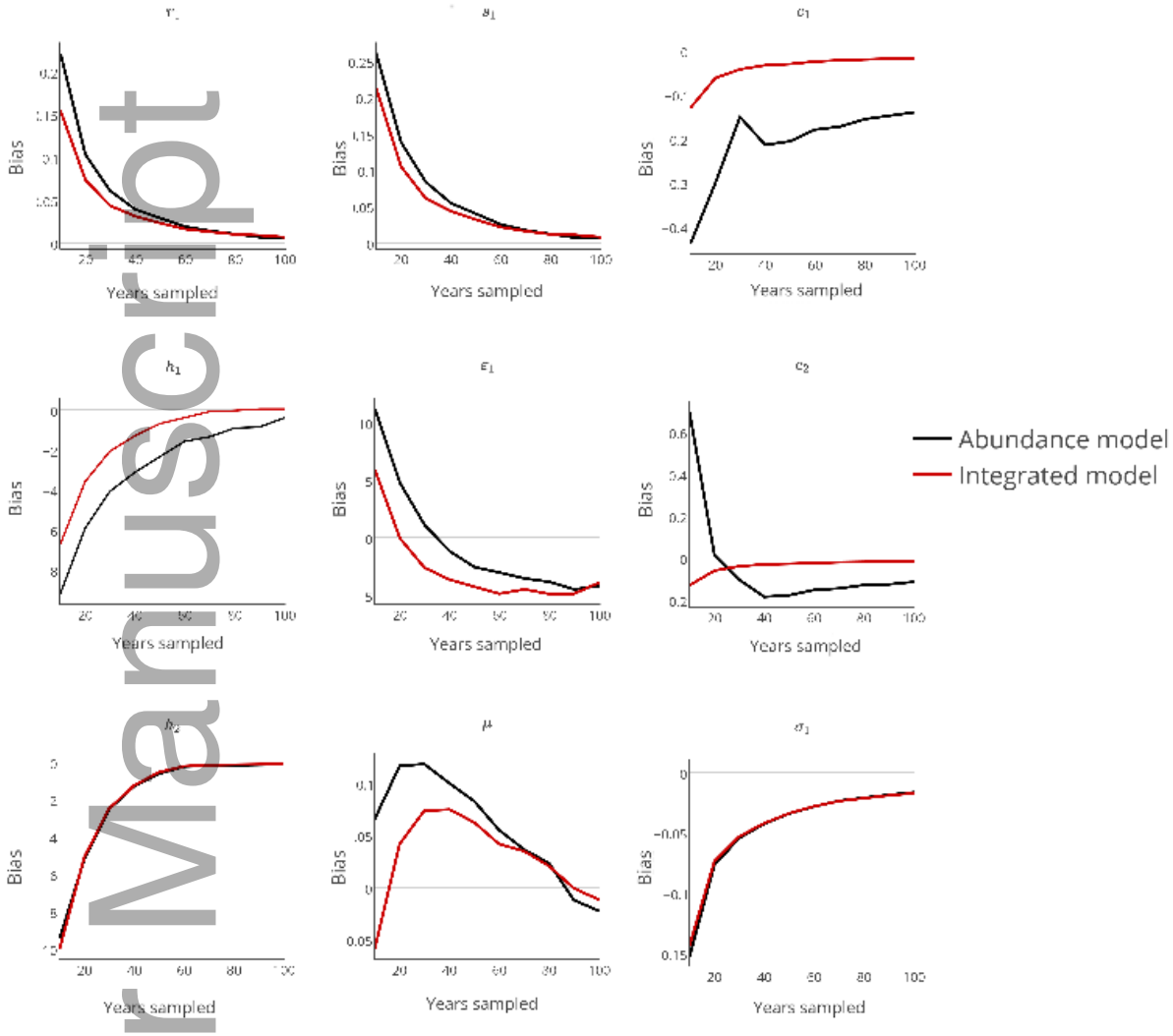

Figure 3: Estimator bias under a type II functional response with high process variance. Parameters ε_2, σ_2, and σ_p are not reported as their behavior is similar to ε_1 and σ_1. Bias is given in terms of the difference between the log parameter values, the x-axis is given in terms of the number of sample points used for the estimation, where samples occur yearly.

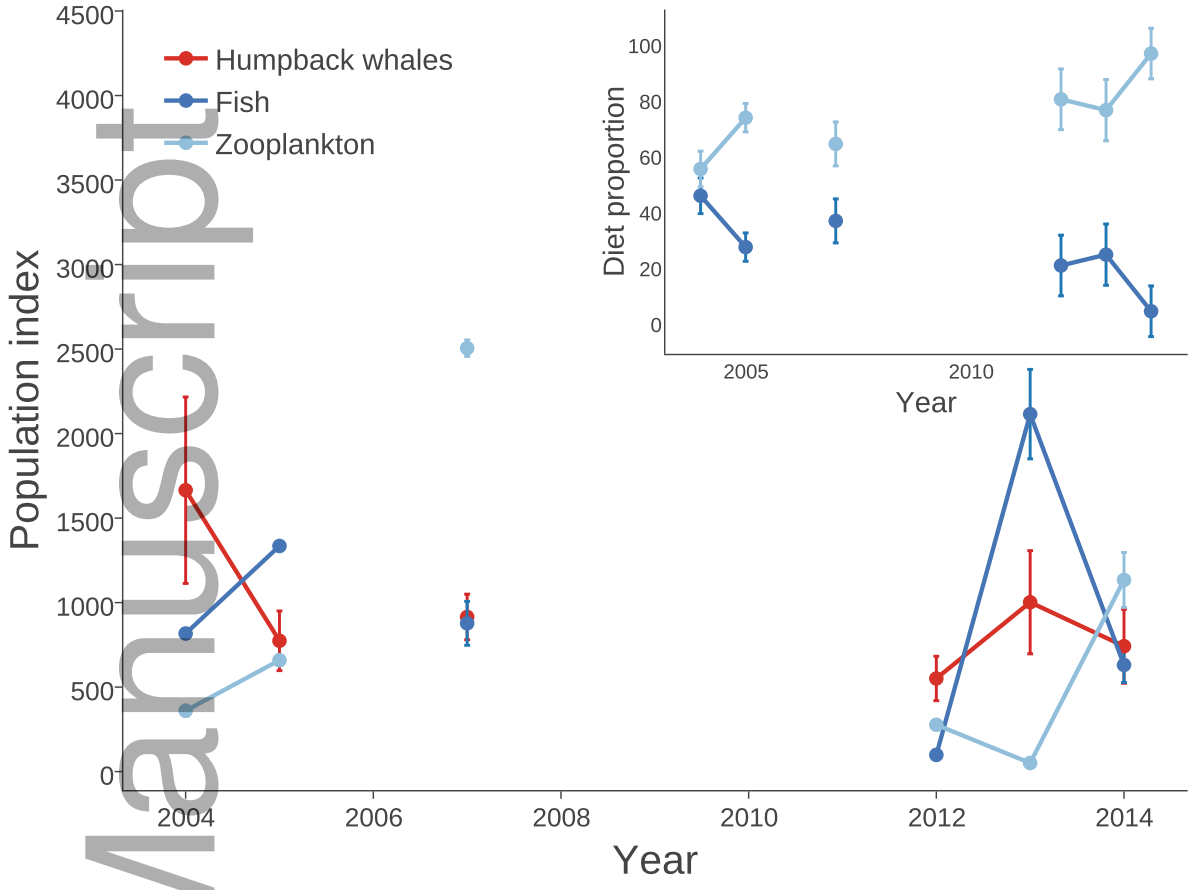

Figure 4: Estimated abundances of humpback whales and their prey from 2004 to 2014. Points denote mean population index estimates, error bars are one standard error from the mean. Proportional diets of whales (inset) are estimated using stable isotopes, thus, are expressed in terms of assimilated biomass. Each point in the inset gives the posterior mean diet estimate and error bars are one posterior standard deviation from the mean.

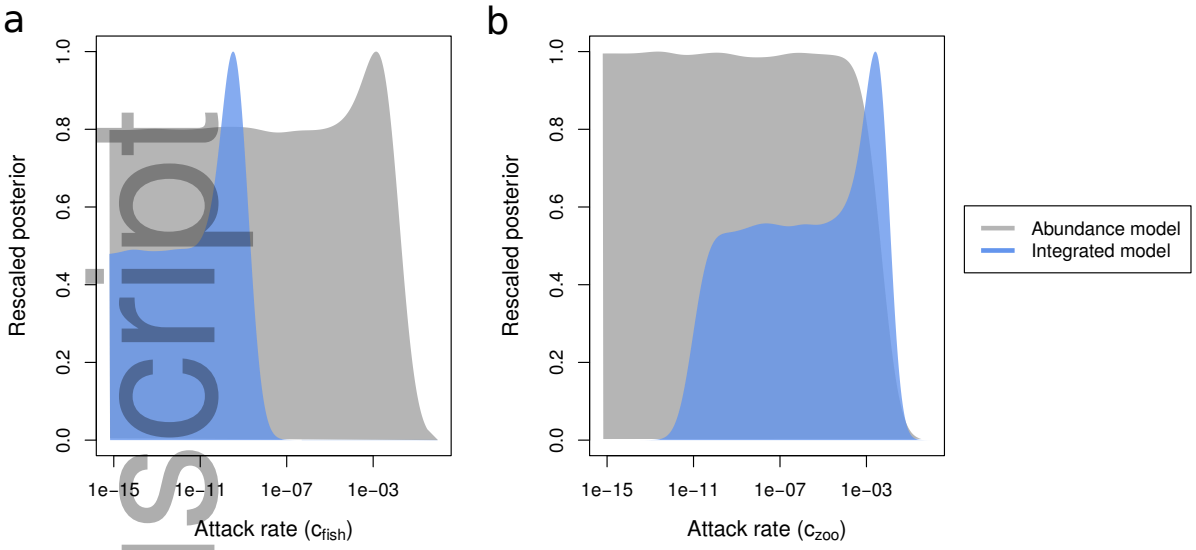

Figure 5: Posterior distribution of interaction rates between humpback whales and their prey. Abundance model in grey, integrated model in blue. Posteriors are rescaled for comparability.

Table 1: Parameters used for simulations.

Parameter	symbol	value
conversion efficiency		
type I and II response	ε_1, ε_2	0.6, 0.6
consumption rate		
type I response	c_1, c_2	0.0002, 0.00024
type II response	c_1, c_2	0.001, 0.003
half-saturation coefficient		
type II response	h_1, h_2	5, 5
predator mortality rate	μ	0.1
prey growth rate	r_1, r_2	1.8, 1.8
strength of prey density dependence	s_1, s_2	0.001, 0.001
process error		
type I and II response	σ_P, σ_1, σ_2	varied

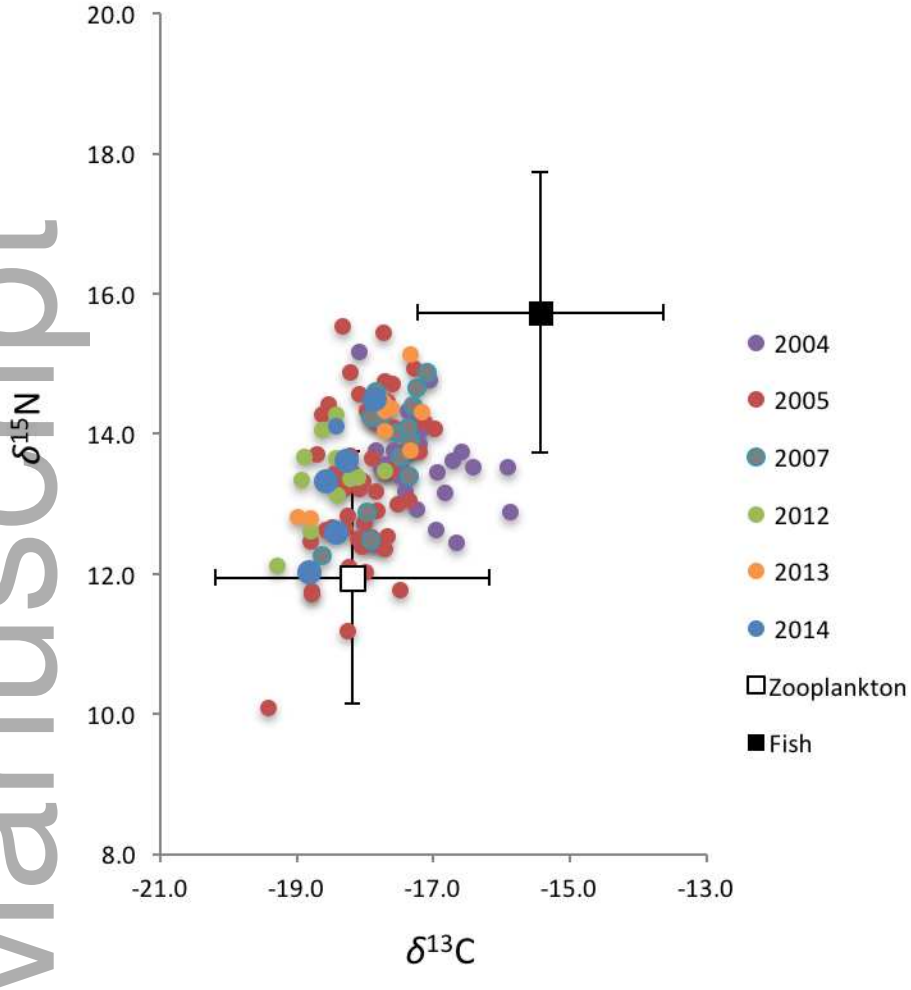

mee3_13001_f1.png

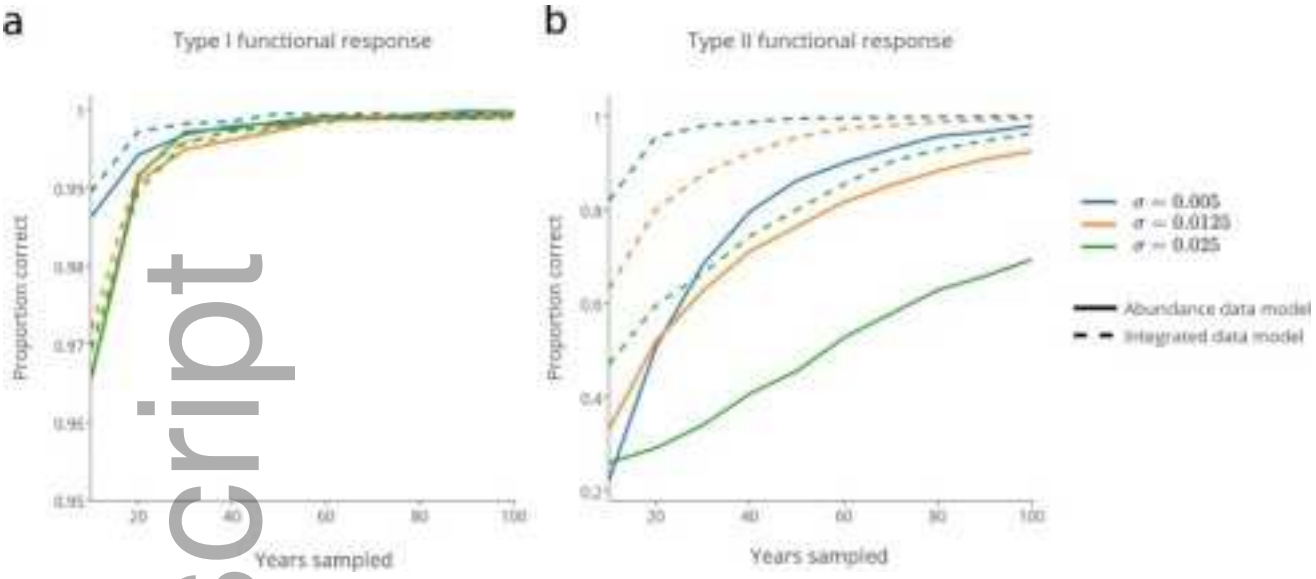

mee3_13001_f2.png

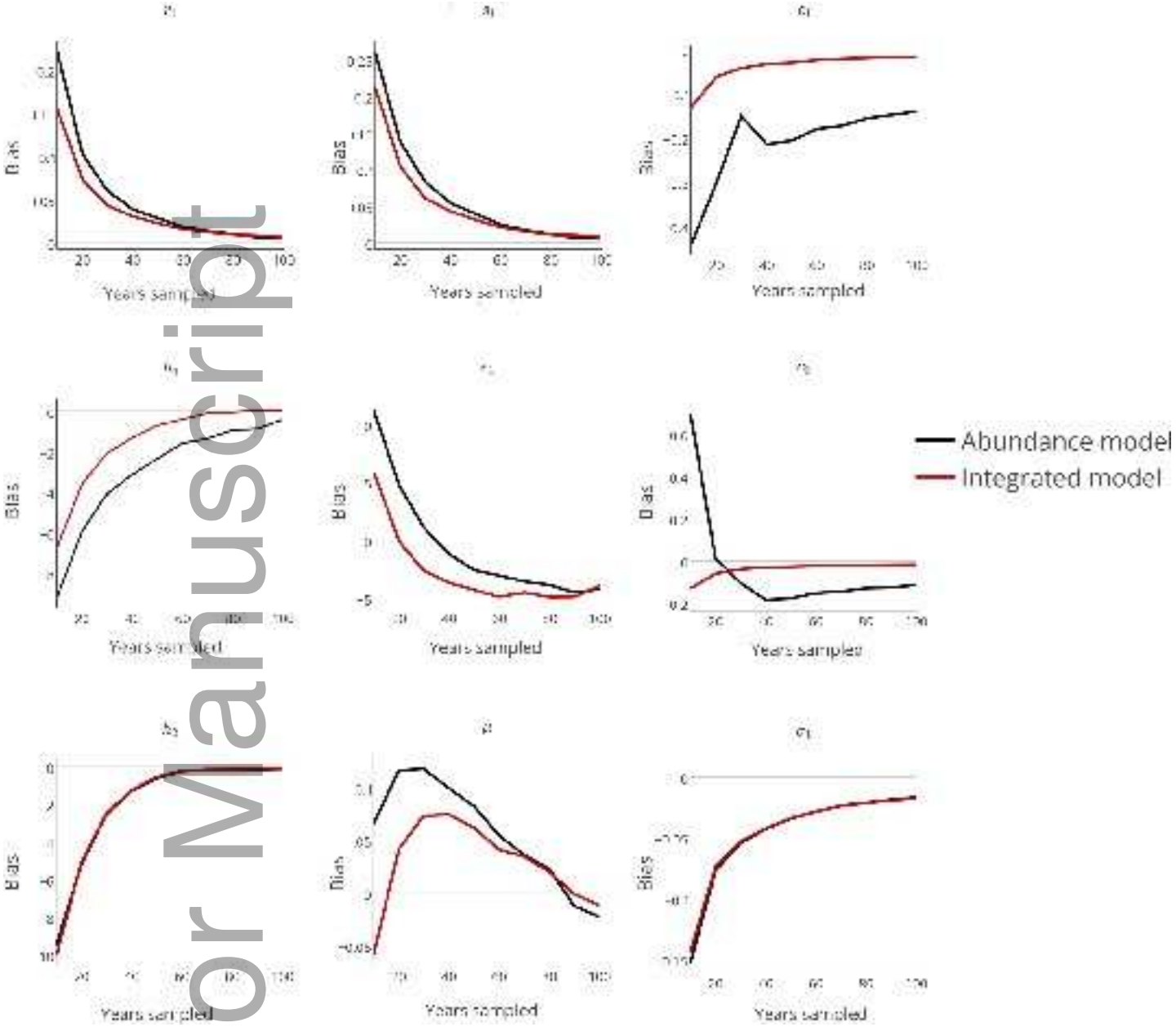

mee3_13001_f3.png